Purification, Cloning, and Functional Characterization of a Novel Immunomodulatory Protein from *Antrodia camphorata* (Bitter Mushroom) That Exhibits TLR2-Dependent NF-κB Activation and M1 Polarization within Murine Macrophages[†]

Fuu Sheu,*,§,‖ Po-Jung Chien,⊥ Kuang-Yang Hsieh,# Kah-Lock Chin,‖ Wan-Ting Huang,‖ Chiao-Yin Tsao,‖ Yin-Fang Chen,‖ Hui-Chung Cheng,‖ and Hui-Hsin Chang‖

§Research Center of Food and Biomolecules and ‖Department of Horticulture, National Taiwan University, Taiwan, Republic of China, ⊥Department of Horticulture and Biotechnology, Chinese Culture University, Taiwan, Republic of China, and #Chi-Mei Medical Center and Hospital, Tainan, Taiwan, Republic of China

A new immunomodulatory protein, designated ACA, was purified from the mycelium extract of *Antrodia camphorata*, a well-known folk medicine bitter mushroom in Taiwan, and N-terminally sequenced. By taking advantage of its N-terminal amino acid sequence, the full-length ACA gene was cloned using rapid amplification of cDNA ends (RACE) approach. This gene encodes a 136 amino acid protein that is homologous to the phytotoxic proteins from fungi. On the basis of the data of N-terminal sequencing and *N*-glycosidase F treatment, the native ACA was confirmed to be a glycoprotein. The similarity in activation of TLR4-deficient macrophages by both the native ACA and recombinant ACA (rACA) suggested that the glycosyl group(s) of the native ACA was insignificant in macrophage activation. Moreover, the failure of rACA to induce TLR2-deficient macrophages and to activate the RAW 264.7 macrophages transfected with the dominate-negative MyD88 (dnMyD88) indicated that the ACA-mediated macrophage activation was TLR2/MyD88 dependent. Microarray assay of the ACA-activated NFκB-related gene expression showed that rACA demonstrated a LPS-mimetic proinflammatory response toward RAW 264.7 macrophages. Furthermore, rACA enhanced phagocytosis activity and CD86 (B7-2) expression as well as induced TNF-α and IL-1β production within murine peritoneal macrophages. A time-dependent induction of mRNA expression of cytokines TNF-α, IL-1β, IL-6, and IL-12 as well as chemokines CCL3, CCL4, CCL5, and CCL10, but not IL-10, CCL17, CCL22, and CCL24, was observed after the ACA treatment of the macrophages. These results proposed that ACA exhibited M1 polarization and differentiation in macrophages. Thus, ACA is an important immunomodulatory protein of *A. camphorata*.

KEYWORDS: Immunomodulatory protein; *Antrodia camphorata*; TLR2; NF-κB; macrophage activation

INTRODUCTION

Bioactive mushroom proteins, mainly identified as agglutinins and lectins, are the most important agents providing diverse antitumor and immunomodulation activities. They can activate lymphocytes and stimulate cell proliferation as well as cytokine secretion in vitro (*1*), stimulate macrophage (*2*, *3*), inhibit the growth of implanted tumor cells (*4*), or cause cytotoxic or immunosuppressive effect in vivo (*5*). These capabilities have

led us to consider it as a potential remedy for treating diseases in various states (*5*, *6*).

Antrodia camphorata grown on the inner cavity of endemic *Cinnamomun kanehirai* Hay is a well-known and highly valued medicinal bitter mushroom in Taiwan and other Oriental countries, but is virtually unknown in the Western world. It has become popular as a folkloric medicine as well as a source of physiologically beneficial mushrooms in Taiwan and has been also reported to inhibit hepatitis and many types of cancer including liver (*7*), lung (*8*), prostate (*9*), and breast (*10*) as well as leukemia (*11*). The capability of *A. camphorata* to modulate the immune system has been studied. Steroid, ergostane, and benzenoid compounds of this mushroom have been reported to possess anti-inflammatory effects (*12*). Moreover, various polysaccharide extracts of *A. camphorata*, obtained from fruiting bodies and cultured mycelia, have been shown to be able to

Article

J. Agric. Food Chem., Vol. 57, No. 10, 2009 **4131**

scavenge free radicals (*13*), to reduce LPS-induced inflammatory reaction in macrophages (*14*), to inhibit the replication of hepatitis B virus (*15*), to suppress the invasion of liver cancer cells (*7*) and tumor growth in hepatoma-bearing mice (*11*), to induce cytokine production and increase the population of CD4(+) T cells (*16*), and also to inhibit the infection of pathogens. Although *A. camphorata* is able to modulate the immune systems, few of its bioactive compounds have been identified and studied.

Microbial components such as lipoglycans, microbial DNA, peptidoglycans, and lipoproteins are known as pathogen-associated molecular patterns (PAMPs). They are recognized by immune cells through the Toll-like receptors (TLRs) (*17*), which in turn induces both innate and adaptive immune responses. The recognition of microbial components by TLR of the macrophages initiates the activation of myeloid differentiation primary response protein (MyD88) (*18*), which is the universal TLR signal adaptor protein. Subsequently, it induces IRAK phosphorylation and TRAF-6 recruitment, which leads to the activation of NF-κB pathway, the release of NF-κB from IκB, and the translocation of NF-κB into nucleus to induce proinflammatory and immune-related gene expression (*18*, *19*). Among the TLRs, TLR2 is known to interact with a large variety of microbial ligands, such as lipoproteins, peptidoglycans, and zymosan from yeast cell wall (*20*, *21*). This interaction allows macrophages to exhibit self-polarization and differentiation to further drive the maturation and development of adaptive immunity (*22*).

Here we report the isolation and characterization of a new immune-regulating agent, designated ACA, from the mycelium extract of *A. camphorata*. Our data showed that ACA is a glycoprotein capable of activating macrophages through a TLR2/MyD88-dependent pathway, hence eliciting proinflammatory response and also arousing the M1 type polarization of the macrophages.

MATERIALS AND METHODS

Materials. *A. camphorata* strain ATCC 200183 was purchased from Bioresource Collection and Research Center, Taiwan (Hsinchu, Taiwan). Fermented mycelium of *A. camphorata* was obtained from the Grape King Inc. Co. (Tou-Yuan, Taiwan). DE-52 cellulose was purchased from Whatman (Maidstone, Kent, U.K.). Mono Q HR 5/5, Superdex 75 10/300 GL gel filtration, and HiTrap Chelating HP columns were purchased from Amersham Biosciences (Uppsala, Sweden). Dialysis membrane tubing (Spectra/Por 1, MWCO 6−8 kDa) was purchased from Spectrum (Rancho Dominguez, CA). Lipopolysaccharide (LPS) from *Escherichia coli* (serotype 0.55:B5), thioglycoslate, and concanavalin A (ConA) were purchased from Sigma Chemical (St. Louis, MO). *N*-Glycosidase F, an N-glycosylation-specific proteinase, was obtained from Takara Bio Inc. (Shiga, Japan). All other chemicals were of analytical grade (Sigma Chemical, St. Louis, MO).

E. coli DH5α (Invitrogen, Carlsbad, CA) was used for nucleic acid manipulations. *E. coli* BL21 was used as the host for expression vector pET32a(+) (Novagen, Madison, WI). All bacterial strains were cultured according to standard procedures. Antibodies against MHC-I, MHC-II, CD80, and CD86 were obtained from eBioscience (Boston, MA). Anti-TLR2 (clone T2.5) antibody was obtained from Hycult Biotechnology (Uden, The Netherlands).

Animals and Cell Line. TLR2 mutation mice (TLR2$^{-/-}$, strain B6.129-Tlr2$^{tm1Kir/J}$), and TLR4 deletion mice (TLR4$^{-/-}$, strain C57BL/10ScN) were purchased from the Jackson Laboratory (Bar Harbor, ME), and C57BL/6J mice were obtained from the Laboratory Animal Center of National Taiwan University (Taipei, Taiwan). Mice were housed in plastic cages in a room maintained at 23 ± 2 °C and $55 \pm 5\%$ humidity with a 12 h light/12 h dark cycle. The mice were fed a standard diet (Rodent Diet 5001; PMI Nutrition International, St. Louis, MO) and had free access to water throughout the experimental period. All animal experiments were approved by the Animal Care and Use Committee of National Taiwan

University. The care and handling of the animals were in accord with internationally recognized guidelines for ethical animal research. Macrophages from C57BL/6J mice were used as wild-type (WT) controls in experiments in which the gene-targeted mice were on the C57BL/6J background.

RAW 264.7 murine macrophage cell line was purchased from the American Type Culture Collection (Manassas, VA). Thioglycollate-elicited macrophages were established from the peritoneal exudates collected from thioglycollate-injected C57BL/6J, TLR2$^{-/-}$ and TLR4$^{-/-}$ mice 4 days after intraperitoneal injection of 1.5 mL of 4% thioglycollate medium as described previously . Peritoneal cavity macrophages were harvested by lavage of the peritoneal cavity with PBS. Peritoneal washings were centrifuged, and then the cells were gently resuspended in 1 mL of RBC lysis buffer (Sigma) for 2 min at room temperature to hemolyze contaminating erythrocytes followed by 9 mL of chilled PBS to restore isotonicity. Subsequently, cells were collected by centrifugation. The cells were suspended and plated onto 96-well flat-bottom plates (5×10^5 cells per well) (Corning) and incubated for 4 h for adherence in a humidified atmosphere of 5% CO_2 at 37 °C. Any nonadherent cells were removed by washing the wells with PBS. The adherent monolayer cells considered as macrophages were further cultured in Dulbecco's modified eagle medium (DMEM) supplemented with 10% (v/v) FBS (Gibco/BRL, Eggenstein, Germany).

Purification of ACA. Fresh *A. camphorata* mycelium (1000 g wet weight) was homogenized with 4 L of 5% (v/v) cold acetic acid and 0.1% (v/v) 2-mercaptoethanol using a BeadBeater machine (BioSpec Products, Inc., Bartlesville, OK). The homogenates were centrifuged at 10000g for 30 min, and soluble proteins in the supernatant were then precipitated by adding ammonium sulfate to 95% of saturation. The precipitates were collected by centrifugation at 15000g for 30 min and were dialyzed extensively against 10 mM Tris buffer (pH 8.2). The dialysate was first fractionated on a Whatman DE-52 cellulose column (2.5 cm × 20 cm) with a 0−1.0 M sodium chloride gradient in 10 mM Tris buffer (pH 8.2). The activity of each fraction was then determined by the stimulatory activity on nitric oxide (NO) production of RAW 264.7 macrophages. The proteins in fractions eluted from 80 and 120 mL (**Figure 1A**) were found to possess activity and were pooled (Supporting Information Figure 1). The pooled protein sample was further fractionated with a Mono Q HR 5/5 column using a 0−1.0 M sodium chloride gradient in 10 mM Tris buffer (pH 8.2). This allowed us to obtain the native ACA with very high homogeneity. Approximately 40−50 mg of ACA was recovered from 1000 g of *A. camphorata* mycelium. All purification procedures were carried out at 4 °C.

The molecular mass of the native ACA was estimated by gel filtration chromatography as described previously (*2*) on a Superdex 75 10/300 GL gel filtration column (1 × 30 cm) using a FPLC system. The column was equilibrated and eluted with a 50 mM phosphate buffer containing 0.15 M NaCl (pH 7.0) at a flow rate of 1 mL/min. The standard proteins (Amersham Biosciences) used for M_r calibration were bovine albumin (M_r 67000), ovalbumin (M_r 43000), chymotrypsinogen A (M_r 25000), and ribonuclease A (M_r 13700). Void volume (V_0) of the column was determined by using blue dextran (1 mg/mL in equilibration buffer). The calibration curve (Supporting Information Figure 2) was obtained by plotting V_e/V_0 (K_{AV}) against their respective logarithmic molecular masses.

Deglycosylation. The deglycosylation of ACA was performed in denatured condition using *N*-glycosidase F enzyme (Takara, Japan) according to the manufacturer's protocols. Briefly, 25 μg of ACA in 2.5 μL was added to 2.5 μL of 1% SDS/0.2 M 2-mercaptoethanol/1 M Tris-HCl (pH 8.6) and heated at 100 °C for 3 min. The denatured ACA was hydrolyzed with *N*-glycosidase F (1 mU) at 37 °C for 20 h, and the product was further analyzed using Tricine sodium dodecyl sulfate−polyacrylamide gel electrophoresis (SDS-PAGE).

Electrophoresis and Amino Acid Sequence Analysis. SDS-PAGE analyses were performed to estimate the molecular mass of native ACA and *E. coli* expressed recombinant ACA (rACA) samples, whereas Tricine SDS-PAGE was used to analyze the deglycosylated ACA sample. The polyacrylamide gels were stained with Coomassie Brilliant Blue R250. The apparent molecular mass was determined using the calibration line plotted from the relative mobility protein standards, consisting of ovalbumin (45000), carbonic anhydrase (30000), trypsin inhibitor (20100), and lysozyme (14300). To detect glycoprotein, the polyacrylamide gels were stained with periodic acid−Schiff (PAS) reagent (Merck, Darmstadt, Germany) .
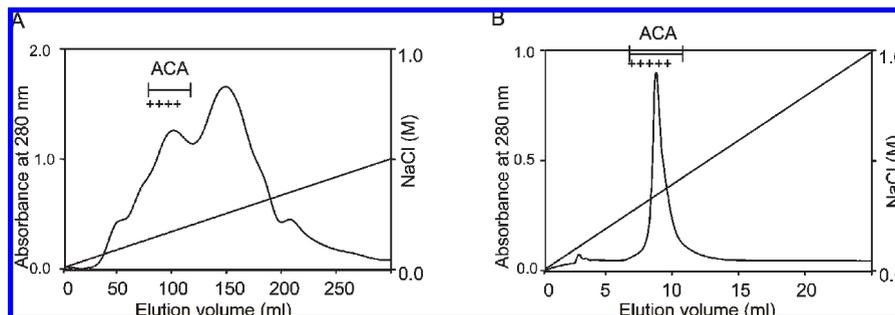
Sheu et al.

Figure 1. Chromatographic isolation and purification of ACA. (**A**) Elution profile of the ammonium sulfate precipitates of *A. camphorata* from a DE-52 cellulose column. The distribution of ACA in the elution profile is indicated by the symbol +. (**B**) Purification of ACA by Mono Q chromatography. The distribution of ACA is indicated by the symbol +. The native ACA has a gel mobility corresponding to a 28.7 kDa protein. The conditions for ACA purification were described under Materials and Methods.

Native ACA sample was separated by SDS-PAGE and electroblotted onto a polyvinylidene difluoride (PVDF) Immobilon P (Millipore) membrane by employing the Trans-Blot Cell system (Bio-Rad) in a transfer buffer. The protein band corresponding to ACA was cut out from the Coomassie Blue-stained membrane and was then subjected to N-terminal-end sequencing. Automated Edman degradation and sequence analysis were carried out on the Applied Biosystems Liquid Pulse Sequencer 476A (Instrument Development Center, National Chung-Hsing University, Taiwan).

RACE-PCR Cloning. In general, standard molecular biology techniques were carried out as described by Sambrook and Russell (*23*). *A. camphorata* was cultured with malt extract agar (Difco) for 3 weeks, and its total RNA was extracted using Qiagen RNeasy Plant Mini Kit (Qiagen, Germantown, MD) according to the manufacturer's recommendation. The first-strand cDNA used as the template for PCR cloning was synthesized from 1 μg of total RNA using the Thermoscript RT-PCR system (Invitrogen). Three prime RACE-PCRs were performed using the 3′-SMART RACE cDNA Amplification Kit (Clontech, Mountain View, CA) and a gene-specific primer PR4 (5′-ACCTACGACCCCTTCTTC-GACAA-3′), which was degenerated from the N-terminal amino acid sequence of ACA. A 618 bp PCR amplification product (PR4-618 fragment) was then cloned into pGEM-T Easy vector (Promega, Madison, WI). After transformation into *E. coli* DH5α, colonies were randomly selected and their plasmid DNA was further extracted and sequenced. The 5′ end of ACA was obtained by using the 5′-SMART RACE cDNA Amplification Kit (Clontech) with a PR14 primer (5′-GTCCCAATTC-GATACTCCTAAAC-3′), designed with the sequence of PR4-618 fragment. A 664 bp PCR product (PR14-664 fragment) was cloned and sequenced using the same method. After the alignment of PR4-618 and PR14-664 fragments, a full-length sequence of ACA cDNA was obtained. This sequence was amplified and confirmed with an independent PCR cloning using gene-specific primers located between the 5′- and 3′-untranslated regions (UTR) of ACA cDNA. The nucleotide sequence of ACA has been deposited in the GenBank database under accession no. AY569691.

Preparation of Recombinant ACA (rACA). The open-reading frame (ORF) of signal peptide reduced ACA (Val^{19}–Arg^{136}) was amplified by PCR with cDNA as a template. The primers PR16 (5′-ATCGG-GATCCGTAAACGTGACCTAT-3′) and PR17 (5′-CACGCTCGAGT-TACAGCCCGCACAC-3′) were used and *Bam*HI/*Xho*I sites were introduced to the 5′ and 3′ ends, respectively. The PCR product was ligated into pGEM-T vector (Promega) and confirmed by DNA sequencing. The insert was excised with *Bam*HI/*Xho*I (Promega) and subcloned into the expression vector pET32a(+), which was previously cut with the same restriction enzymes, to generate pET32/ACA. The rACA was expressed as a fusion protein (Trx−ACA) with an 18 kDa Trx-Tag thioredoxin at the end of the N-terminal.

E. coli BL21 transformed with pET32/ACA was used to overexpress rACA. The procedure was modified to obtain soluble recombinant protein. Briefly, an overnight culture was diluted 1:100 with Luria−Bertani (LB) broth and grown at 37 °C until the absorbance at 600 nm reached 0.6. Final concentration of 0.5 mM isopropyl-β-D-thiogalacto-pyranoside (IPTG) was added. After a further shaking culture for 3 h to

induce rACA production, the rACA expressed by bacteria was harvested by centrifugation. Cell supernatant containing the fusion protein Trx−ACA was then prepared after the treatment of ligase buffer, sonication, and centrifugation.

N-Terminal Trx-tagged rACA was purified from the cell supernatant by a HiTrap Chelating HP column (Amersham Biosciences). The clear supernatant was 1:10 diluted with a binding buffer (20 mM sodium phosphate, 500 mM NaCl, pH 7.4) and subjected to the HiTrap Chelating HP column. The column was gradually washed with washing buffer (5−100 mM immidazole in binding buffer) and then eluted with elution buffer (100−500 mM immidazole in binding buffer). Purified Trx−ACA, solvated in cleavaging buffer (20 mM Tris-HCl, pH 7.4, 50 mM NaCl, 20 mM CaCl$_2$), was further hydrolyzed with Entrokinase (Amersham Biosciences) to remove Trx-Tag from rACA. Finally, the rACA was purified using a Mono Q HR 5/5 column again with the method described previously. The purity of rACA was analyzed using 12% SDS-PAGE, and protein concentration was determined according to the method of Bradford with bovine serum albumin as a standard.

Measurement of Nitric Oxide and Cytokine Production. Chromatographically eluted *A. camphorata* fractions, native ACA, and purified rACA samples were dissolved in PBS for cell experiments. RAW 264.7 or murine peritoneal macrophages (5 × 10^5 cells/well in a 96-well plate) were activated with various concentrations of ACA protein (0−50 μg/mL) alone and were incubated for 24 h. The cultured soups were collected to evaluate the amount of nitric oxide (NO), TNF-α, and IL-1β produced by the macrophages. The levels of accumulated nitrite (NO$_2^-$) in cell-free supernatants were determined using the colorimetric Griess reaction (*24*) to estimate the amount of NO released by macrophages. Mouse cytokines TNF-α and IL-1β in culture supernatants were determined by commercial sandwich ELISA sets (BD PharMingen, San Jose, CA) according to the manufacturer's recommendation.

Fluorescence-Activated Cell Sorting (FACS). For detecting the expression of surface MHC-I, MHC-II, CD80, and CD86, murine peritoneal macrophages were treated with ACA samples at 37 °C for 24 h. The macrophages were then collected in PBS followed by resuspension with PBS containing 2% bovine serum albumin and 0.1% sodium azide (FACS buffer). Suspended cells were washed twice in FACS buffer and stained with unconjugated primary antibody specific for MHC-I, MHC-II, CD80, or CD86 (eBioscience, San Diego, CA) at 4 °C for 30 min. Subsequently, cells were washed twice with FACS buffer and incubated with FITC conjugated secondary antibody at 4 °C for 30 min. Cells were washed again with FACS buffer, and the resuspended cells were then acquired on a FACScan (BD Biosciences, Franklin Lakes, NJ) to perform analysis using CellQuest software (BD Biosciences). The results are expressed in total mean fluorescence intensity (MFI) and percentage of positive fluorescent cells. Cells incubated only with the secondary antibody served as negative controls. Data analyses were performed by comparison of peak fluorescence intensities between the control and treated groups. Phagocytosis activity was determined using a Phagocytosis analysis kit (Nihon Gene Research Laboratories, Sendai, Japan) according to the manufacturer's protocol.

Microarray Analysis of NFκB Signaling Pathway. The Oligo GEArray Mouse NFκB Signaling Pathway Microarray (SuperArray

Article

J. Agric. Food Chem., Vol. 57, No. 10, 2009 **4133**

Bioscience, Frederick, MD) was used to detect the ACA-induced signaling pathway in RAW 264.7 macrophages, and hybridization procedures were performed according to the manufacturer's instructions. Macrophage cells were treated with or without rACA (20 μg/mL) or with LPS (1 μg/mL) as a positive control, and total RNA was extracted after 4 h of incubation using the TRIzol reagent following the manufacturer's instructions. Three micrograms of total RNA was reverse-transcribed into the biotin-16-dUTP-labeled cRNA probe with biotin-16-uridine-5′-triphosphate (Roche) using the TrueLabeling-AMP linear RNA amplification kit (SuperArray) according to the manufacturer's instructions. The Super-Array membrane (OMM-025) was prehybridized at 60 °C for at least 2 h. Hybridization of the biotin-labeled cRNA probe (6 μg) to the membrane was carried out at 60 °C overnight under slow agitation in a hybridization oven. The hybridized membrane was washed with saline sodium citrate buffer once in solution I (2× SSC, 1% SDS) and again in solution II (0.1× SSC, 0.5% SDS) at 60 °C for 15 min each. The membrane was blocked with GEAblocking solution Q (SuperArray) for 40 min and incubated with alkaline phosphatase-conjugated streptavidin for 10 min at room temperature. For detection, chemiluminescent reaction was performed using CDP-Star substrate. Images were obtained using the ChemiGenius chemiluminescence detection system (Syngene, Cambridge, U.K.) and analyzed with the Web-based GEArray Expression Analysis Suite software (SuperArray). The relative expression level of each gene was estimated by comparing its signal intensity normalized to internal control GAPDH.

Real-Time PCR for mRNA Quantification. Cells were homogenized in TRIzol reagent (Invitrogen), and total RNA was isolated from the homogenate according to the manufacturer's instructions, with the use of chloroform extraction and isopropanol precipitation. The integrity and quality of RNA samples were checked on 0.5% TBE agarose gels. The concentrations of RNAs were determined by using a NanoDrop ND-1000 spectrophotometer (NanoDrop Technologies, Wilmington, DE). All RNA samples had a 260/280 absorbance ratio between 1.8 and 2.1. The first-strand cDNA was synthesized from the total RNA as a template using ThermoScript RT-PCR system (Invitrogen) for evaluating gene expression involved in the ACA-mediated immunomodulation in macrophages. Briefly, 3 μg of total RNA was mixed with 1 μL of dNTP mix and 1 μL of oligo(dT)$_{20}$ at 65 °C for 5 min. Subsequently, the RNA was reverse-transcribed in a final 20 μL reaction volume using 4 μL of cDNA synthesis buffer, 1 μL of DTT, 1 μL of RNaseOUT, and 15 units of ThermoScript reverse transcriptase at 50 °C for 50 min. The reaction was then terminated by incubation at 85 °C for 5 min. The cDNA was treated with RNase H to remove RNA complementary to the cDNA prior to the PCR. Each RT-PCR was repeated three times using independent RNA extracts and cDNA synthesis reactions.

Differential expression for individual genes was assessed by quantitative real-time PCR (qPCR). For PCR amplification, specific primer sets were designed for SYBR Green probes with Roche Probe Design Software (Roche) based on macrophage-related cytokine and immune factor sequences on NCBI. β-Actin or GAPDH (endogenous gene) was used to confirm the quality of reverse-transcribed cDNA, and previous PCR products or genomic DNA were used as internal controls. qPCR was performed on the Applied Biosystems 7300 Real-Time PCR System (Applied Biosystems, Foster City, CA) in a final volume of 25 μL in each well containing 5 μL of diluted cDNA, 1 μL of dNTP (10 mM), 2.5 μL of 10× PCR buffer (200 mM Tris-HCl, pH 8.4, and 500 mM KCl), 1 μL of MgCl$_2$ (50 mM), 1 μL of sense- and antisense-specific oligonucleotide primers (10 μM each), 0.5 μL of ROX reference dye, 0.025 μL of diluted SYBR Green dye, and 0.5 unit of *Taq* DNA polymerase (Invitrogen). PCR conditions were carried out according to the manufacturer's protocol consisting of an initial denaturation step of 95 °C for 10 min, followed by 40 cycles with denaturation at 95 °C for 15 s and a combined annealing/elongation step at 56 °C for 1 min. No-template controls were included in each real-time run for each primer set. Using real-time PCR platforms, dissociation curves spanning 56−95 °C generated a melting curve to detect primer dimer interference and unspecific PCR products and to confirm melting profiles of amplicons. Samples were run in triplicates in separate wells to permit the quantification of the target sequences normalized to endogenous genes. The expression level of each target gene was quantified by the relative levels of a given mRNA according to cycling threshold (Ct) analysis.

Establishment of Dominant Negative MyD88 in RAW 264.7 Macrophages. According to the method modified from Burns (*25*), the mouse MyD88 cDNA was obtained by reverse transcription PCR (Invitrogen) using the total RNA isolated from the mouse RAW 264.7 cell line as a template, to generate overexpressed and dominant-negative (dn) MyD88-expressing clones. MyD88 (full-length, GenBank accession no. BC058787) and dnMyD88 (amino acids 161−296) cDNA fragments were cloned separately into pGEM-T Easy vector (Promega) using the following oligonucleotides as primers: 5′-end of MyD88, 5′-AATTGG-TACC**ATG**TCTGCGGGGAGACC-3′; 3′-end of MyD88, 5′-GAATTCT-CAGGGCAGGGACAAAGCC-3′; 5′-end of dnMyD88, 5′-GCCTGGT-ACCT**ATG**GATGCCTTTATCTGC-3′; 3′-end of dnMyD88, 5′-GAA-TTCTCAGGGCAGGACAAAGCC-3′. Recognition sites for restriction enzymes are underlined; **boldface** nucleotides denote the start (5′-end oligonucleotides) and stop codons (3′-end oligonucleotides). Following transformation into *E. coli* DH5α by heat shock, positive clones were identified by blue-white selection on LB agar plates containing 100 μg/mL ampicillin, 0.5 mM IPTG, and 40 μg/mL X-Gal followed by insert-specific PCR testing. The purified plasmid DNA using the Mini-M plasmid extraction system (Viogene) was digested with *Kpn*1 and *Eco*R1 according to the primers incorporating restriction enzyme sites and was inserted into *Kpn*1 and *Eco*R1-digested pcDNA3.1 (+) using T4 DNA ligase (New England BioLabs) to generate pcDNA3.1-MyD88 and pcDNA3.1-dnMyD88, respectively.

RAW 264.7 cells reaching 50% confluence in 24-well culture plates were used for transfection with FuGENE 6 Transfection Reagent (Roche) according to the manufacturer's instructions. To normalize the transfection efficiency, β-galactosidase activity from the cotransfected with pCMV-βGal plasmid as the internal control of the cells was measured using a mammalian β-galactosidase assay kit (Pierce) following the manufacturer's instructions. After 48 h of incubation, RAW 264.7 cells were further stimulated with rACA (10 μg/mL) and LPS (1 μg/mL) for 20 h to determine the production of TNF-α of the cells. All transfection experiments were carried out in triplicate, repeated at least three times, and normalized for β-galactosidase activity.

Data Analysis. Data are presented as mean ± SD of three separate experiments performed in triplicates (n = 3). Statistical analysis was made by means of Student's *t* test and one-way ANOVA. Differences were considered to be statistically significant when the P value was below 0.05 ($P < 0.05$).

RESULTS

Chromatographic Purification of ACA. To isolate the putative bioactive protein (designated ACA, an abbreviation of <u>A</u>ntrodia <u>c</u>amphorata <u>a</u>gent), a DE-52 anion-exchange chromatography with a linear salt gradient (0−1.0 M NaCl, 10 mM Tris buffer, pH 8.2) was first used to fractionate the proteins in the ammonium sulfate precipitate (95% saturation) of *A. camphorata* mycelium extract (**Figure 1A**). The lack of agglutination signal for all of the tested samples implied that ACA is neither a lectin nor an agglutinative glycoprotein (data not shown). To locate the protein fractions with immunomodulatory functions, all of the fractionated samples were analyzed for their capabilities to induce NO production within murine macrophage cell line RAW 264.7. As shown in **Figure 1A**, the protein samples obtained from the elution volume of 80−120 mL possessed NO-stimulating activity (Supporting Information Figure 1). The ACA-containing protein samples were then pooled and precipitated with ammonium sulfate before being subjected to further purification by Mono Q anion-exchange chromatography. A major protein peak was achieved after gradient elution of the ion-exchange column (**Figure 1B**). This peak contained only a single detectable protein band with gel mobility corresponding to a 27 kDa protein after SDS-PAGE and staining with periodic acid/Schiff reagent (**Figure 2A**). The brilliant purple color of this protein band suggested that the native ACA is a glycoprotein.

Molecular Cloning of ACA. The native ACA separated on SDS−polyacrylamide gel was electroblotted onto a PVDF

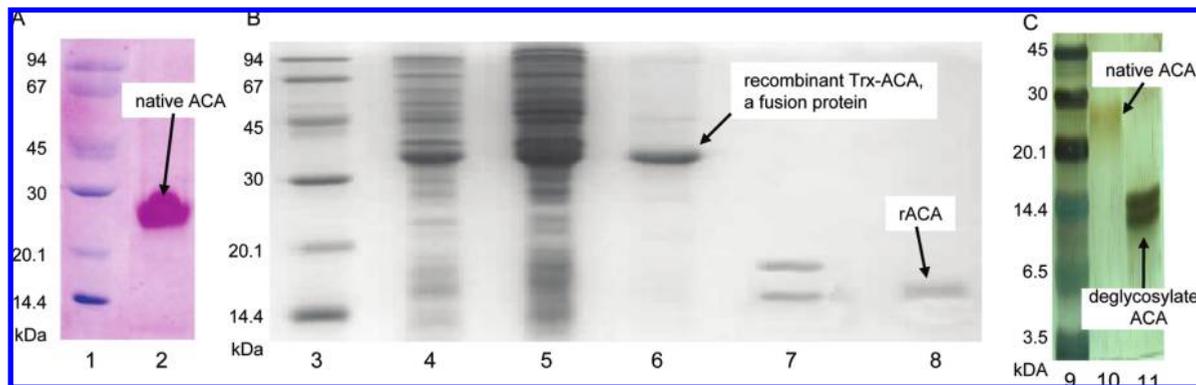**4134** *J. Agric. Food Chem.,* Vol. 57, No. 10, 2009

Sheu et al.

Figure 2. Electrophoretic analyses for native ACA, recombinant ACA (rACA), and deglycosylated ACA. (**A**) Migration of native ACA in SDS-polyacrylamide gel. The gel was stained with periodic acid/Schiff solution. The position of native ACA (in red) is indicated. (**B**) Migration of Trx−ACA and rACA in SDS−polyacrylamide gel. (**C**) Mobility of deglycosylated ACA in SDS−polyacrylamide gel. Lanes: 1 and 3, molecular mass markers; 2 and 10, native ACA; 4, noninduced *E. coli* lysate; 5, IPTG-induced *E. coli* lysate; 6, imidazole-eluted Trx−ACA fusion protein; 7, entrokinase digested products of Trx−ACA; 8, purified rACA; 9, Amersham peptide markers; 11, deglycosylated ACA.

membrane, recovered, and then subjected to N-terminal amino acid sequence analysis. The sequence of the most N-terminal 27 amino acid residues was V-VTYDPFFDNPPNNLLYYAA-SSDDTN, which showed rare similarity to any known protein as revealed by the Blast search on NCBI database. In addition, the inability of the second amino acid residue of native ACA to be identified suggested that it might be a site of modification.

Taking advantage of the N-terminal amino acid sequence of the native ACA, RACE strategy was adopted to clone the ACA gene and allowed us to obtain a DNA fragment with a length of 618 bp (PR4-618). The N-terminal amino acid sequence of one of the open reading frames (ORF) of this DNA had 78% identity to that of the sequenced native ACA (Supporting Information Figure 3A). On the basis of these results, the PR4-618 was regarded as a candidate for the 3′-portion of the ACA gene. To synthesize the full-length cDNA of ACA, a primer (PR14) with a sequence from nucleotide position 511 to 533 of the PR4-618 fragment was designed and used to perform the 5′-RACE PCR reaction, by which another 664 bp DNA fragment (PR14-664) was achieved. The 19th and 21st amino acid residues (Val[19] and Val[21]) encoded by PR14-664 were identical to those of the sequenced native ACA (Supporting Information Figure 3B). After the corresponding two ORFs of PR4-618 and PR14-664 had been merged, the cDNA sequence of ACA was obtained. It was 738 bp in length and contained a 453 bp ORF that encodes a 136 amino acid ACA precursor (**Figure 3**).

Homology of ACA to Phytotoxic Proteins from Fungi. Amino acid sequence comparison among ACA and known phytotoxic proteins from fungi revealed that they are homologous. ACA shared 62% identity with a hypothetical protein from *Gibberella zeae* PH-1 (XP_391381.1) in the Cerato-platanin phytotoxin region. It also shared more than 40% identity with the snodprot1 protein precursor from *Neurospora crassa* (XP_328493) and *Phaeosphaeria nodorum* (O74238), secreted protein 1 from *Leptosphaeria maculans* (AAM33130), Cerato-platanin of *Ceratocystis fimbriata* f. sp. *platani* (CAC84090), an antigen from *Coccidioides posadasii* (CS-Ag, AAN73410), and an allergen precursor Asp f 15 (O60022) from *Aspergillus fumigatus* (Supporting Information Figure 4).

ACA Contains a Signal Peptide and Is Glycosylated. The first 18 amino acid residues were predicted to form a signal peptide (possibility of ~0.90), which may be cleaved during the maturation or secretion of ACA. The finding that the native ACA began with a Val residue (Val[19]) at its N-terminus supported this idea (Supporting Information Figure 5).

To characterize the functions of ACA in greater detail, the cDNA sequence corresponding to this part of ACA was cloned into a pET-32a(+) vector and yielded a Trx−ACA fusion protein when expressed in *E. coli* BL21. On the basis of the coding sequence of rACA, it had a molecular mass of only 12.2 kDa, which was 16.5 kDa much smaller than that proposed for the native ACA (28.7 kDa). Because rare modification of recombinant protein was found in prokaryotic expression system, we proposed that the difference in molecular masses between the native ACA and rACA resulted from the modification of native ACA.

To search for the modification sites on native ACA, glycosylation prediction of ACA with NetNGly 1.0 software was first conducted. Our results revealed that Asn[20] of the full-length ACA had the highest possibility ($P = 0.8053$) to be N-glycosylated, followed by Asn[31] and Asn[87] ($P = 0.6351$ and 0.6668, respectively). However, low potential of O-glycosylation of ACA was found with the YingOYang 1.2 Prediction. Thus, ACA might be glycosylated mainly through *N*-glycosyl bonds. To confirm this idea, the native ACA was hydrolyzed with *N*-glycosidase F, a specific N-glycosylation protease, and the deglycosylated protein was analyzed with SDS-PAGE. As shown in **Figure 2C**, the deglycosylated ACA had a molecular mass of approximately 12 kDa, which was similar to that of rACA. The ability of the native ACA to be cleaved by *N*-glycosidase F clearly demonstrated that the native ACA contained carbohydrate moieties.

ACA Directly Activates the NF-κB Signaling Pathway in Murine Macrophages. The induction level of TNF-α in the cultured soups was then determined using ELISA. As shown in **Figure 4A**, both the native ACA and rACA (0.026−1.480 μM) showed dose-dependent induction of TNF-α in the macrophages, although the level of TNF-α induction was higher in response to rACA than to native ACA. Similar inductions were observed for IL-1β and NO by the presence of ACA (data not shown). These results indicated that rACA shared similar functions with native ACA and that rACA could replace native ACA for further functional analyses of ACA. Besides the test on the RAW 264.7 macrophages, the effects of ACA on immune response of murine peritoneal macrophages were also examined. Our data showed that rACA (10 μg/mL) quickly induced a high level of TNF-α 1 h after incubation with murine peritoneal macrophages; however, the level of TNF-α decreased 12 h after the induction (**Figure 4B**). In contrast, rACA relatively delayed IL-1β production by murine peritoneal macrophages.

```
  1    acg cgg gga taa cac tca aga gtc agg tag ctc tgc gat acc gga    45

 46    gac ctc agc caa cca act gcc ttc cgt tcc aca ata gcc ATG AAG    90
                                                            M   K

 91    GTC GCT GTC GCC CTC AGT GCT CTC TTC CTC CTT CCC TCC GCT CTC   135
  3     V   A   V   A   L   S   A   L   F   L   L   P   S   A   L    17

136    GGT GTA AAC GTG ACC TAT GAC CCT TTT TTT GAC AAC CCA AAC AAC   180
 18     G   V   N   V   T   Y   D   P   F   F   D   N   P   N   N    32

181    TCT CTC AGC TAC GTC GCT TGC TCG GAT GGT ACC AAT GGT CTT CTC   225
 33     S   L   S   Y   V   A   C   S   D   G   T   N   G   L   L    47

226    ACC AAA GGG TAT ACC ACC TTG GGC TCC CTC CCT GAT TTC CCT TAC   270
 48     T   K   G   Y   T   T   L   G   S   L   P   D   F   P   Y    62

271    ATT GGA GGC GCA TAT GCC ATC GCA GGA TGG AAT TCC CCG AGC TGT   315
 63     I   G   G   A   Y   A   I   A   G   W   N   S   P   S   C    77

316    GGC ACA TGT TGG GAG CTA ACA TAC AAC AAC GTC AGC ATC AAC ATA   360
 78     G   T   C   W   E   L   T   Y   N   N   V   S   I   N   I    92

361    TTG GGG ATC GAC ACA GCT GCG GGC TTC AAC ATT GCA CTT ACG GCT   405
 93     L   G   I   D   T   A   A   G   F   N   I   A   L   T   A   107

406    ATG AAC GTA CTC ACC AAT AAC GCG GCC GTA GAT CTG GGG GAG GTT   450
108     M   N   V   L   T   N   N   A   A   V   D   L   G   E   V   122

451    GAT GCA GCG GCA ATA CAG GTC GAC TCG TCC GTG TGC GGG CTG TAA   495
123     D   A   A   A   I   Q   V   D   S   S   V   C   G   L   *   137

496    aga tat gta aaa cag ctg gaa att tgt gga cga tgt cat atg tca   540

541    tca ttt tgg act cgt ggc ata gtt gaa act gat gcc tag tgt gtc   585

586    att aaa gtc tct tgt tac cac caa aca atg ctc gac gtg aga tcg   630

631    tgg gga gaa tgt ttg att gtt tag gag tat cga att ggg aca aat   675

676    tta aac ata aaa aaa aaa aaa aaa aaa gaa aaa aaa aac aaa aaa   720

721    aaa aaa aaa aaa aaa aaa                                       765
```

Figure 3. Complete nucleotide sequence of the cDNA encoding ACA and its deduced amino acid sequence. The amino acid residues in the coding sequence of ACA are in capital letters. The underlined amino acid residues (Val[19]−Leu[138]) represent the mature part of ACA and *E. coli* expressed rACA. The amino acid residues used for designing PR4 primer (used for 3′ RACE) are indicated by bold and italic letters.

The murine peritoneal macrophages began to increase IL-1β secretion only 8 h postincubation with rACA (10 μg/mL) (**Figure 4C**). These results demonstrated that ACA activated the RAW 264.7 cell line and murine peritoneal macrophages in both dose- and time-dependent manners.

The effect of rACA (10 μg/mL) on the murine phagocytotic activity was investigated using flow cytometry assays. By comparison with the control cells (**Figure 4D**, dark line, MFI 18.01), rACA effectively enhanced the phagocytotic activity of murine peritoneal macrophages (**Figure 4D**, dotted line, MFI 25.11). The expressions of class II major histocompatibility complex (MHC-II) as well as costimulatory molecules B7.1 and B7.2 (CD80 and CD86, respectively) by rACA-induced murine macrophages were also evaluated. Our results showed that rACA was able to increase the expression of CD86 (**Figure 4E**, red line) and MHC-II (**Figure 4F**, red line) but not CD80 (data not shown), suggesting that ACA only partly enhanced the presentation capability of macrophages.

It has been shown that the expression of TNF-α was correlated well with the activation of NF-κB pathway in macrophage cells (*26*). Therefore, a microarray analysis using an Oligo GEArray Mouse NF-κB Signaling Pathway kit was carried out to investigate the NFκB-related gene activation in RAW 264.7 macrophages by rACA (20 μg/mL). **Figure 5** shows the gene expression profile of the rACA-induced RAW 264.7 macrophages, and the profile was similar to that induced by LPS (100 ng/mL). Moreover, the genes induced by rACA 1-fold higher than the control

were also identical to those stimulated by LPS (**Table 1**). Clearly, ACA exhibited a LPS-mimetic activity in murine macrophages.

Involvement of TLR2 and MyD88 in ACA Activation. The similarity in the gene expression profiles of the macrophages induced by rACA and by LPS which activated macrophage through TLR4 and subsequent MyD88 and STAT6 caspases suggested that the TLR was involved in the ACA-mediated signaling. The involvement of TLR4 in the rACA-mediated macrophage activation was first examined. As shown in **Figure 6A**, the defect of TLR4 (TLR4$^{-/-}$) did not interrupt the activation of C57BL/10ScN peritoneal macrophages by rACA. Similar results were found in the activation of TLR4$^{-/-}$ macrophages from C57BL/10ScN mouse by native ACA (data not shown). On the contrary, neutralization of TLR2 with antimouse TLR2 mAb, prior to incubation with rACA, significantly inhibited the TNF-α production in C57/B6 peritoneal macrophages (**Figure 6B**). Moreover, rACA (1−50 μg/mL) failed to activate the TLR2-defective (TLR2$^{-/-}$) macrophages from B6.129-Tlr2$^{tm1Kir/J}$ mouse (**Figure 6C**). These results indicated that TLR2, rather than TLR4, was involved in the recognition of ACA.

The involvement of MyD88 in ACA signaling was proven through the use of a dominant-negative MyD88 mutant of RAW 264.7 macrophage. In the analysis, MyD88 or truncated MyD88 was overexpressed in macrophage by liposomal transfection of MyD88 or by transfection with pcDNA3.1($+$) plasmid harboring the dnMyD88 gene, respectively. As shown in **Figure 6D**,
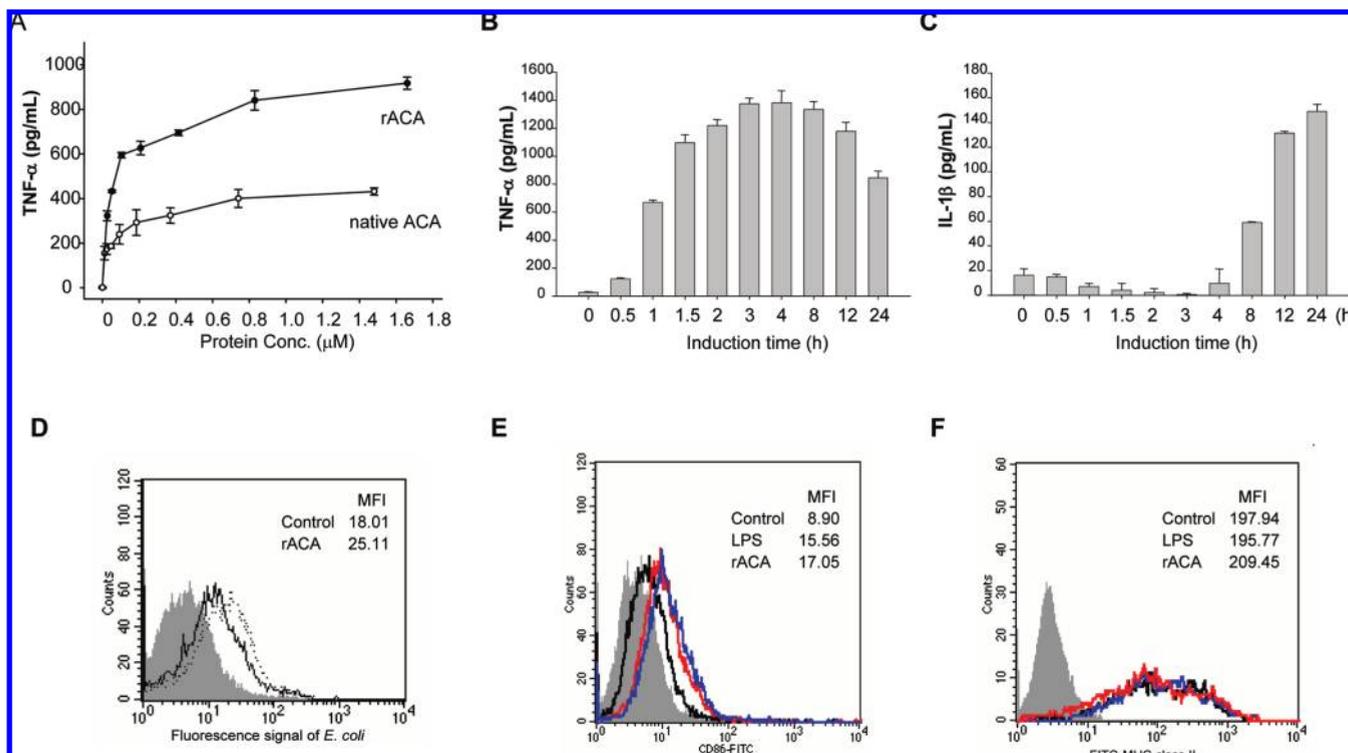
Figure 4. Activation of murine macrophages by ACA. The cells were cultured in the presence of ACA samples for 24 h. (**A**) Dose-dependent induction of TNF-α in RAW 264.7 macrophages by native ACA (○) and rACA (●). (**B**, **C**) TNF-α and IL-1β production, respectively, by rACA-induced (10 μg/mL) murine peritoneal macrophages. The TNF-α and IL-1β levels were determined using ELISA. (**D**, **E**, **F**) Phagocytosis activity, CD86, and MHC class II expression, respectively, within rACA-activated (10 μg/mL) murine peritoneal macrophages. The phagocytosis activity, CD86, and MHC class II expression were determined using FACS methods described under Materials and Methods.
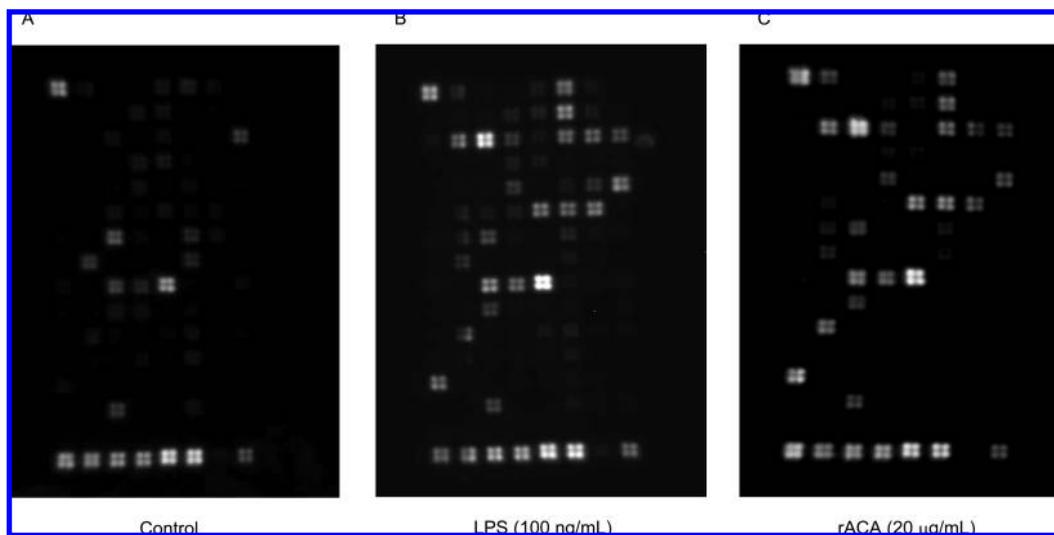

Figure 5. Gene expression profile of murine RAW 264.7 macrophages treated with ACA. (**A**, **B**, **C**) Profiles of control cells, 100 ng/mL LPS-treated cells, and 20 μg/mL rACA-treated cells, respectively, identified using Oligo GEArray NF-kB Signaling Pathway microarray. The overexpressed NFκB-related genes are listed in **Table 1**.

a 52.2% decrease in TNF-α production was observed when the truncated MyD88 was transfected into RAW 264.7 cells, by comparison with that of the MyD88-transfected control. The reduction in ACA activation by the decrease in effective MyD88 suggested the involvement of MyD88 in the ACA-mediated macrophage activation.

Induction of Cytokine mRNA Expression and M1 Polarization in Murine Macrophages. After investigation of the signaling pathway of ACA, we further evaluated the ability of ACA to enhance the mRNA expression of macrophage-producing cytokines and

chemokines using real-time quantitation PCR technique. As shown in **Figure 7**, rACA (10 μg/mL) greatly increased the mRNAs of TNF-α, IL-1β, IL-6, IL-12, and iNOS but not that of IL-10 in murine peritoneal primary macrophages. During the first hour of induction, rACA aroused a 12-fold TNF-α mRNA production in comparison with that in the noninduced control cells (**Figure 7A**); however, the induction decreased thereafter. A 50-fold increase in IL-6 mRNA production was also observed during the second hour of induction (**Figure 7C**), but full induction of IL-1β, iNOS, and IL-12 expresssion required a longer time

Article

J. Agric. Food Chem., Vol. 57, No. 10, 2009 **4137**

Table 1. Selection and Category of Overexpressed NFκB-Related Genes in RAW 264.7 Macrophages Investigated by Oligo Gearray Mouse NFκB Signaling Pathway Microarray[a,b]

category and gene name	gene symbol	GenBank accession no.	fold change (rACA-induced)	fold change (LPS-induced)
activation of the NFκB pathway				
EDAR (ectodysplasin-A receptor)-associated death domain	Edaradd	XM_147719	3.25	3.16
inhibitor of κB kinase ε	IKK-I	NM_019777	1.63	1.48
mucosa-associated lymphoid tissue lymphoma translocation gene 1	Malt1	NM_172833	1.75	1.60
NFκB responsive genes				
colony-stimulating factor 2 (granulocyte−macrophage)	GM-CSF	NM_009969	4.02	3.35
colony-stimulating factor 3 (granulocyte)	G-CSF	NM_009971	4.26	4.29
interleukin 6	IL-6	NM_031168	1.59	1.61
interferon regulatory factor 1	IRF-1	NM_008390	2.75	2.48
tumor necrosis factor α	TNFα	NM_013693	3.39	2.56
other factors involved in the NFκB pathway				
thymoma viral proto-oncogene 1	AKT-1	NM_009652	1.99	1.30
B-cell leukemia/lymphoma 3	BCL-3	NM_033601	1.68	1.93
chemokine (C−C motif) ligand 2	Scya2	NM_011333	3.15	3.83
dual specificity phosphatase 1	Ptpn16	NM_013642	2.36	2.14
endothelial differentiation, lysophosphatidic acid G-protein-coupled receptor 2	Gpcr26	NM_010336	2.39	3.19
interleukin 1 β	IL-1β	NM_008361	2.61	3.63
Jun oncogene	c-JUN	NM_010591	3.23	2.76
LPS-induced TN factor	Pig7	NM_019980	2.29	2.93
mitogen activated protein kinase kinase kinase 14	NIK	NM_016896	1.54	1.01
nuclear factor of κ light polypeptide gene enhancer in B-cells 2, p49/p100	NFκB2	NM_019408	1.58	1.58
solute carrier family 20, member 1	Slc20a1	NM_015747	2.34	1.56

[a] Discrepancy between the initial signals and repeated signal = 1. [b] Multiple genes are plotted in this array; the representative one is listed.
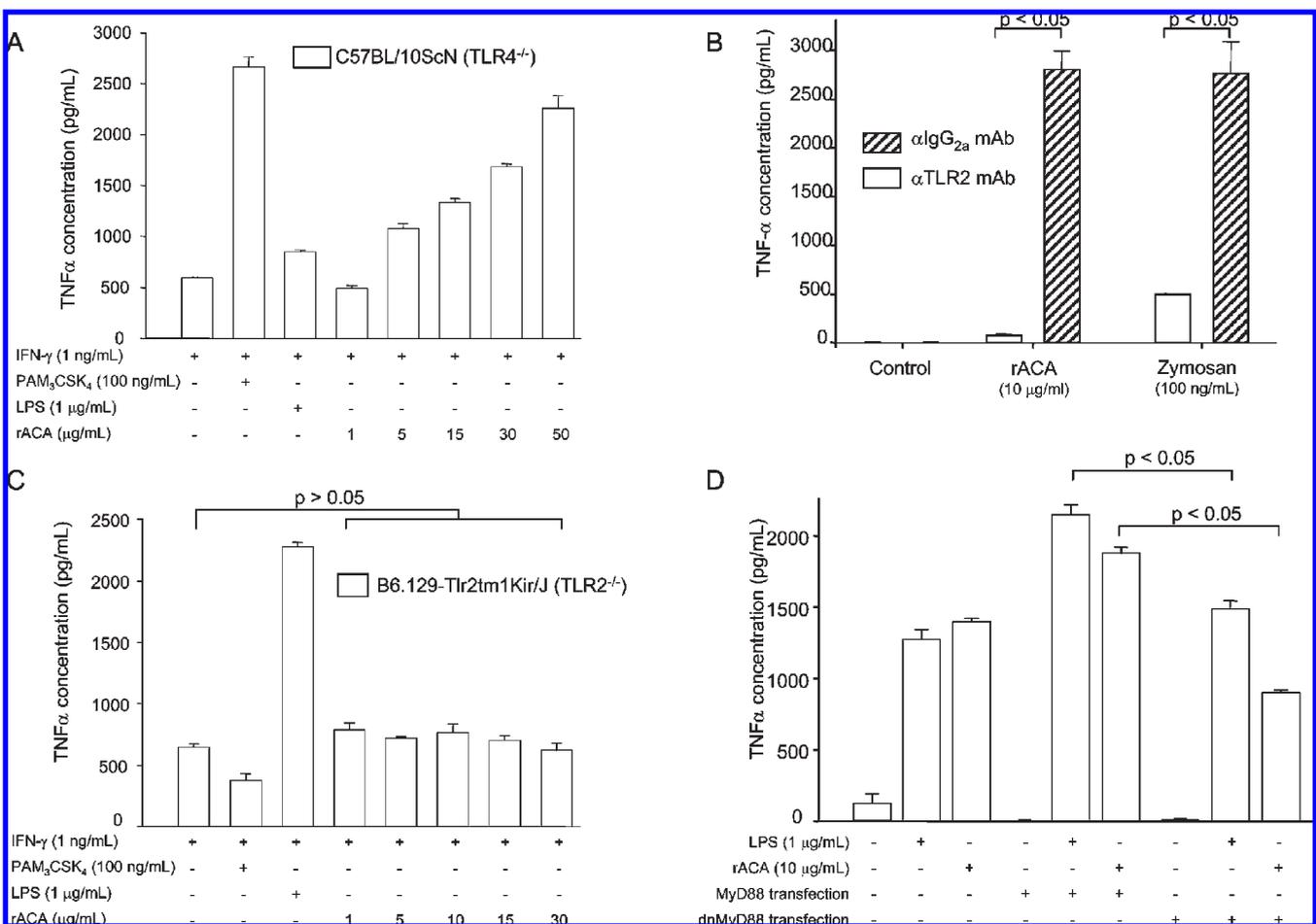

Figure 6. Association of ACA-mediated activation of murine macrophages with TLR2 but not TLR4: (**A**) rACA-mediated activation of C57/10SCN (TLR4$^{-/-}$) peritoneal macrophages; (**B**) inhibition of rACA-mediated activation of C57BL/6 cells by anti-TLR2 mAb; (**C**) failure of rACA to activate B6.129-Tlr2$^{tm1Kir/J}$ (TLR2$^{-/-}$) macrophages; (**D**) rACA-mediated activation of RAW 264.7 macrophages transfected with MyD88 or truncated-MyD88 (dnMyD88). The data shown are representative averages of three independent experiments (*n* = 3).
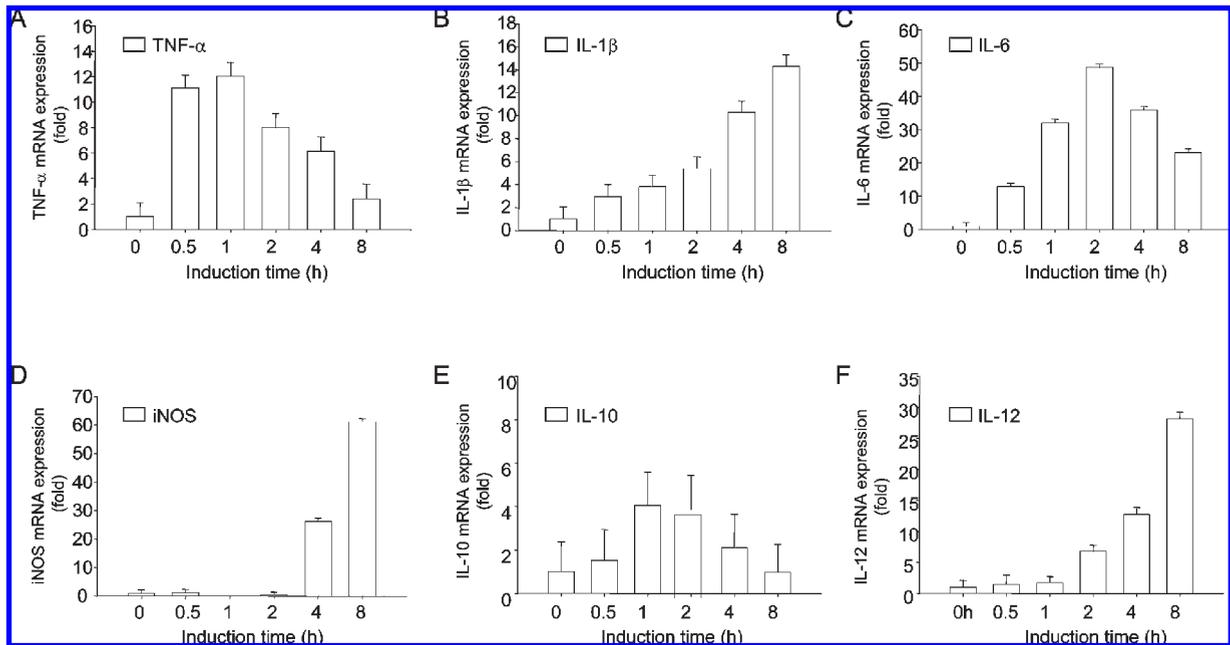
Figure 7. Time course evaluation of ACA-induced mRNA expression of cytokines and iNOS by murine peritoneal macrophages: (**A**−**F**) mRNA expression of TNF-α, IL-1β, IL-6, iNOS, IL-10, and IL-12, respectively, within rACA-induced (10 μg/mL) mouse peritoneal macrophages. The expression levels were determined using quantitative real-time PCR. Levels of mRNA expressions were calculated on the basis of the Ct value and shown as the ratio of each mRNA to that of β-actin. The relative mRNA expression during the time course was presented by dividing the ratio of each mRNA at the specific time point to that at the zero time (0 h). The data shown are representative averages of three independent experiments (n = 3).
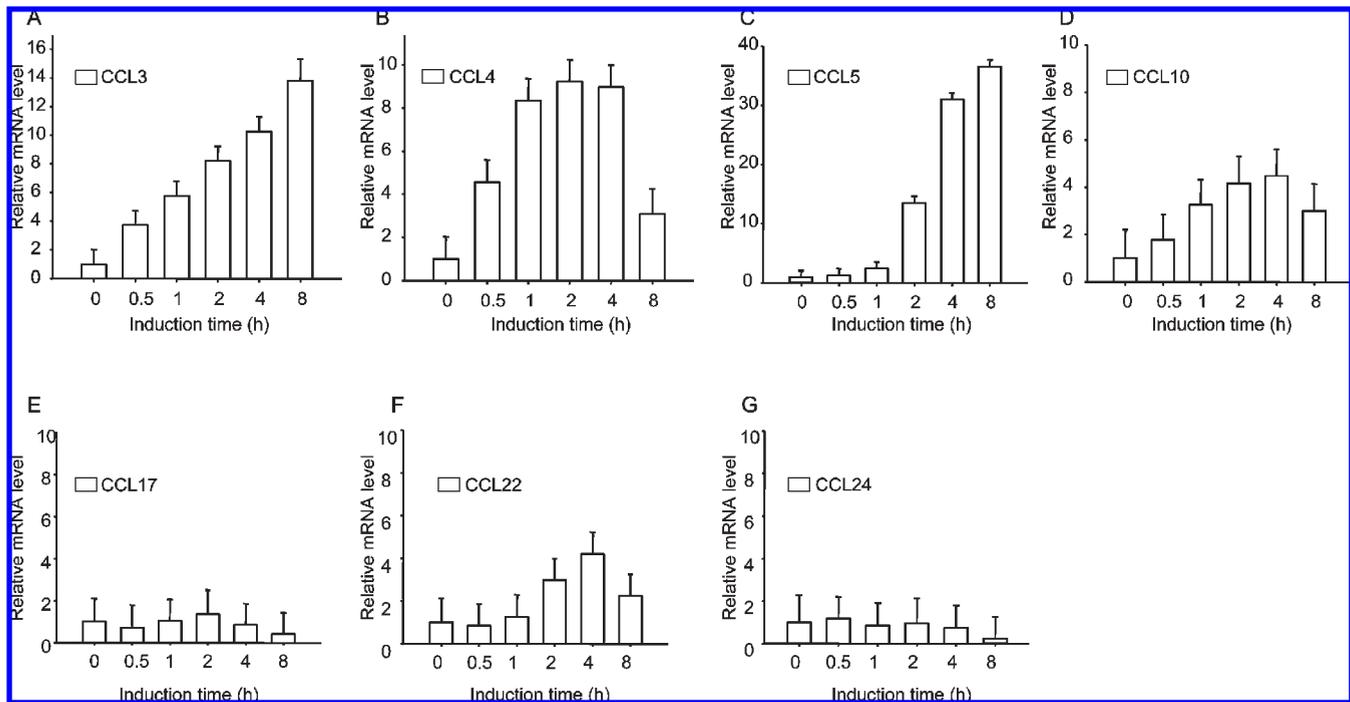

Figure 8. Time course evaluation on ACA-induced mRNA expression of chemokines by murine peritoneal macrophages: (**A**−**G**) mRNA expression of CCL3, CCL4, CCL5, CCL10, CCL17, CCL22, and CCL24, respectively, within rACA-induced (10 μg/mL) mouse peritoneal macrophages. The expression levels were determined using quantitative real-time PCR. Levels of mRNA expressions were calculated on the basis of the Ct value and shown as the ratio of each mRNA to that of β-actin. The relative mRNA expression during the time course was presented by dividing the ratio of each mRNA at the specific time point to that at the zero time (0 h). The data shown are representative averages of three independent experiments (n = 3).

(**Figure 7B,D,F**), and no significant induction of IL-10 mRNA was detected during the rACA activation.

The profiles of ACA-mediated cytokine production, including the enhancement of TNF-α and IL-12, suggested that rACA was capable of enhancing the expression of M1-type chemokines but not those of M2-type. rACA induced macrophage activations in 8 h and significantly (P < 0.05) aroused the mRNA production of M1-type chemokines, including CCL3, CCL4, CCL5, and CCL10 (**Figure 8A**−**D**). On the other hand, none of the M2-type chemokines such as CCL17, CCL22, and CCL24 were activated

Article

J. Agric. Food Chem., Vol. 57, No. 10, 2009   **4139**

by rACA (**Figure 8E−G**). These results demonstrated that ACA activated the M1-type polarization in macrophages, which in turn leads to the Th1-type differentiation in T lymphocytes.

DISCUSSION

We have for the first time identified an immunomodulatory glycoprotein, ACA, from *A. camphorata* and cloned the corresponding gene. The ACA protein contains a signal peptide and N-linked carbohydrate moieties. It not only shows homology to phytotoxic proteins from fungi but also exhibits a marked immune-modulating function in activating murine macrophages. To our knowledge, no phytotoxin-like fungal protein has ever been reported to regulate the immune response in mammalians.

As demonstrated by biochemical and genetic analyses, the native ACA is composed of two major parts: (1) 12.2 kDa peptide moiety (Val^{19}−Leu^{136}) and (2) carbohydrate moieties covalently linked to the peptide part through N-glycosylation as evidenced by the ability of *N*-glycosidase F to cleave away all of the possible carbohydrate moieties (**Figure 2C**). ACA is different from other known macrophage-activating proteins of mushrooms, including the immunomodulatory proteins of *Auricularia polytricha* (*2*) and *Pleurotus citrinopileatus* (*3*), which lack glycosylation. The second amino acid residue (Asn^{20}) of the mature ACA is believed to be a major site for N-glycosylation. This could be substantiated by the highest possibility ($P = 0.8053$) of this amino acid residue to be N-glycosylated as predicted by the NetNGly computer program and by the lack of a significant and specific amino acid signal in the second Edman degradation cycle during the N-terminal sequencing of native ACA. However, the corresponding signals for the first (Val^{19}) and third (Val^{21}) amino acid residues of the native ACA were very distinct (Supporting Information Figure 6).

Hemagglutination analysis and database comparison revealed that ACA was distinct from common lectins, a family of carbohydrate-binding proteins, which cause agglutination of blood cells or function as pattern recognition molecules for pathogens in innate immunity (*27*). This was because neither the chromatographic ACA-containing fractions nor the purified ACA (1−1000 μg/mL, data not shown) exhibited hemagglutinating activity toward red blood cells of human and murine. Furthermore, the addition of some simple sugars such as glucose, galactose, mannose, fructose, and sialic acid into the culture medium (above 1 M in final concentration) was unable to block and influence murine macrophage activation (data not shown). Moreover, the amino acid sequence of ACA was basically different from any known lectin of plants and fungi as revealed by BLAST searching on GenBank. Consequently, we proposed that the ACA-binding molecule on the macrophage surface was not a carbohydrate.

Many proteins homologous to ACA have been found in symbiotic and saprogenic fungi; they include SnodProt1 proteins (expressed by a red bread mold *Neurospora crassa* and plant pathogen *Phaeosphaeria nodorum*) (*28*), sp1 (secreted by *Leptosphaeria maculans* during infection of rapeseed (*Brassica napus*)) (*29*), Cerato-platanin (a phytotoxic protein to induce necrosis in tobacco leaves from a plant-cankerous fungus *Ceratocystis fimbriata*) (*30*), CS-Ag (a major allergen of the fungus *Coccidioides immitis* causing San Joaquin Valley fever) (*31*), and Asp 15 (the pathogenic and allergenic filamentous fungus *Aspergillus fumigatus*) (*32*). The homologues of ACA from *N. crassa* (ccg-14) and *L. maculans* (sp1) are functionally associated with the circadian clock and light regulated (*29*, *33*). Moreover, Cerato-platanin, an ACA homologue of *C. fimbriata*, has an amino acid sequence similar to that of the clock-controlled hydrophobin, Certo-ulmin (*34*, *35*). Although the ACA obtained from Basidiomycota may have a different physiological function from its

homologues from Ascomycota, it may be also secreted to act as a phytotoxic protein because it possesses a predicted signal peptide, which may direct the post-translational transport. Actually, the ACA homologue of *B. napus*, sp1, has been reported to secret and to cause an autofluorescence response toward the host plant (*29*). Nevertheless, not much information on the genomics of basidiomycota related to *Antrodia* are available, and it is noted that the physiological function of ACA in *A. camphorata* deserves further investigation and more work remains to be done before conclusive genome mining for products of this medicinal basidiomycete is feasible.

Our results revealed that ACA is an immune modulator that directly enhanced the major functions of macrophages. It augments the expression of CD86, an important costimulatory molecule for antigen presentation and T lymphocyte activation, which in turn leads to the increases of phagocytosis capability and production of various cytokines and mediators such as TNF-α, IL-1β, IL-6, IL-12 and inducible nitric oxide synthase. IL-12 and TNF-α are associated with the polarized type I responses of the activated M1 macrophages and could further promote the macrophage-mediated adaptive immunity as well as the orientation of adaptive response in a type 1 direction. Moreover, the ACA-induced macrophages express some distinct repertoires of inflammatory chemokines such as macrophage inflammatory protein (MIP)-1α (CCL3), MIP-β (CCL4), and RANTES (CCL5), which are known to be associated with the polarized type I response in macrophages (*22*). Therefore, ACA can be classified as a macrophage stimulant that is able to induce M1 type polarization and strengthen the innate immunity of the host.

The mammalian TLRs, especially TLR2, are responsible for the recognition of microbial products and play important roles in innate immunity (*36*). Various bacterial proteins such as synthetic lipoprotein (Pam$_3$Cys) (*37*), peptidoglycan from *Staphylococcus aureus* (*38*), and outer surface protein A of *Borrelia burgdorferi* (*39*) have been reported to be recognized by TLR2. Our demonstration that the ACA-mediated macrophage activation is blocked by anti-TLR2 mAb and by TLR null mutation ($TLR2^{-/-}$) indicates that TLR2 is indeed the major receptor for the recognition of ACA by macrophage. However, it remains unclear whether ACA is directly recognized by TLR2 or the recognition requires other accessory molecules. Furthermore, the reduced ACA-mediated TNF-α production in the dominant-negative MyD88 mutant of RAW 264.7 macrophages indicates that MyD88 is involved in the ACA-mediated TLR pathway (*18*). The NF-κB activation as well as the enhanced LPS-mimetic gene expression aroused by ACA support that ACA is able to trigger TLR2-mediated downstream signaling through MyD88. Upon stimulation, MyD88 is able to activate IRAK by phosphorylation and then associates with TRAF6, leading to the activation of effector kinases and to the activation of NF-κB (*18*, *19*). On the basis of the above logic and our results, we propose that the protein moiety of ACA is responsible for the interaction with TLR2 and that the TLR2 signaling further triggers NF-κB activation through MyD88 and causes the expression of pro-inflammatory cytokines and chemokines genes.

ABBREVIATIONS USED

ACA, *Antrodia camphorata* agent; rACA, recombinant *Antrodia camphorata* agent; PAMPs, pathogen-associated molecular patterns; MyD88, myeloid differentiation primary response protein; RACE, rapid amplification of cDNA ends; NO, nitric oxide; IL, interleukin; CCL, chemokine (C−C motif) ligand; MFI, mean fluorescence intensity; CD, cluster of differentiation; MHC, major histocompatibility complex.

4140   *J. Agric. Food Chem.,* Vol. 57, No. 10, 2009

Sheu et al.

ACKNOWLEDGMENT

Supporting Information Available: Additional figures. This material is available free of charge via the Internet at http://pubs.acs.org.

LITERATURE CITED

(1) Sze, S. C.; Ho, J. C.; Liu, W. K. *Volvariella* volvacea lectin activates mouse T lymphocytes by a calcium dependent pathway. *J. Cell Biochem.* **2004**, *92* (6), 1193–1202.

(2) Sheu, F.; Chien, P. J.; Chien, A. L.; Chen, Y. F.; Chin, K. L. Isolation and characterization of an immunomodulatory protein (APP), from the Jew's Ear mushroom *Auricularia polytricha. Food Chem.* **2004**, *87* (4), 593–600.

(3) Sheu, F.; Chien, P. J.; Wang, H. K.; Chang, H. H.; Shyu, Y. T. New protein PCiP from edible golden oyster mushroom (*Pleurotus citrinopileatus*) activating murine macrophages and splenocytes *J. Sci. Food Agric.* **2007**, *87* (8), 1550–1558.

(4) Yang, N.; Tong, X.; Xiang, Y.; Zhang, Y.; Liang, Y.; Sun, H.; Wang, D. C. Molecular character of the recombinant antitumor lectin from the edible mushroom *Agrocybe aegerita. J. Biochem.* **2005**, *138* (2), 145–150.

(5) Jeurink, P. V.; Noguera, C. L.; Savelkoul, H. F.; Wichers, H. J. Immunomodulatory capacity of fungal proteins on the cytokine production of human peripheral blood mononuclear cells. *Int. Immunopharmacol.* **2008**, *8* (8), 1124–1133.

(6) De Mejia, E. G.; Prisecaru, V. I. Lectins as bioactive plant proteins: a potential in cancer treatment. *Crit. Rev. Food Sci. Nutr.* **2005**, *45* (6), 425–445.

(7) Hsu, Y. L.; Kuo, P. L.; Cho, C. Y.; Ni, W. C.; Tzeng, T. F.; Ng, L. T.; Kuo, Y. H.; Lin, C. C. *Antrodia cinnamomea* fruiting bodies extract suppresses the invasive potential of human liver cancer cell line PLC/PRF/5 through inhibition of nuclear factor κB pathway. *Food Chem. Toxicol.* **2007**, *45* (7), 1249–1257.

(8) Wu, H.; Pan, C. L.; Yao, Y. C.; Chang, S. S.; Li, S. L.; Wu, T. F. Proteomic analysis of the effect of *Antrodia camphorata* extract on human lung cancer A549 cell. *Proteomics* **2006**, *6* (3), 826–835.

(9) Chen, K. C.; Peng, C. C.; Peng, R. Y.; Su, C. H.; Chiang, H. S.; Yan, J. H.; Hsieh-Li, H. M. Unique formosan mushroom *Antrodia camphorata* differentially inhibits androgen-responsive LNCaP and -independent PC-3 prostate cancer cells. *Nutr. Cancer* **2007**, *57* (1), 111–121.

(10) Hesu, Y. C.; Chen, S. C.; Chen, H. C.; Liaw, J. W.; Yang, H. L. *Antrodia camphorata* inhibits proliferation of human breast cancer cells in vitro and in vivo. *Food Chem. Toxicol.* **2008**, *46* (8), 2680–2688.

(11) Liu, J. J.; Huang, T. S.; Hsu, M. L.; Chen, C. C.; Lin, W. S.; Lu, F. J.; Chang, W. H. Antitumor effects of the partially purified polysaccharides from *Antrodia camphorata* and the mechanism of its action. *Toxicol. Appl. Pharmacol.* **2004**, *201* (2), 186–193.

(12) Shen, C. C.; Wang, Y. H.; Chang, T. T.; Lin, L. C.; Don, M. J.; Hou, Y. C.; Liou, K. T.; Chang, S.; Wang, W. Y.; Ko, H. C.; Shen, Y. C. Anti-inflammatory ergostanes from the basidiomata of *Antrodia salmonea. Planta Med* **2007**, *73* (11), 1208–1213.

(13) Hseu, Y. C.; Chen, S. C.; Yech, Y. J.; Wang, L.; Yang, H. L. Antioxidant activity of *Antrodia camphorata* on free radical-induced endothelial cell damage. *J. Ethnopharmacol.* **2008**, *118* (2), 237–245.

(14) Wu, Y. Y.; Chen, C. C.; Chyau, C. C.; Chung, S. Y.; Liu, Y. W. Modulation of inflammation-related genes of polysaccharides fractionated from mycelia of medicinal basidiomycete *Antrodia camphorata. Acta Pharmacol. Sin.* **2007**, *28* (2), 258–267.

(15) Lee, I. H.; Huang, R. L.; Chen, C. T.; Chen, H. C.; Hsu, W. C.; Lu, M. K. *Antrodia camphorata* polysaccharides exhibit anti-hepatitis B virus effects. *FEMS Microbiol. Lett.* **2002**, *209* (1), 63–67.

(16) Cheng, P. C.; Hsu, C. Y.; Chen, C. C.; Lee, K. M. In vivo immunomodulatory effects of *Antrodia camphorata* polysaccharides

(17) Kaisho, T.; Akira, S. Critical roles of Toll-like receptors in host defense. *Crit. Rev. Immunol.* **2000**, *20* (5), 393–405.

(18) Akira, S.; Hoshino, K.; Kaisho, T. The role of Toll-like receptors and MyD88 in innate immune responses. *J. Endotoxin Res.* **2000**, *6* (5), 383–387.

(19) O'Neill, L. A. The role of MyD88-like adapters in Toll-like receptor signal transduction. *Biochem. Soc. Trans.* **2003**, *31* (Pt 3), 643–647.

(20) Kirschning, C. J.; Schumann, R. R. TLR2: cellular sensor for microbial and endogenous molecular patterns. *Curr. Top. Microbiol. Immunol.* **2002**, *270*, 121–144.

(21) Goodridge, H. S.; Underhill, D. M. Fungal recognition by TLR2 and dectin-1. *Handb. Exp. Pharmacol.* **2008**, *183*, 87–109.

(22) Mantovani, A.; Sica, A.; Sozzani, S.; Allavena, P.; Vecchi, A.; Locati, M. The chemokine system in diverse forms of macrophage activation and polarization. *Trends Immunol* **2004**, *25* (12), 677–686.

(23) Sambrook, J.; Russell, D. W. *Molecular Cloning: A Laboratory Manual*; Cold Spring Harbor Laboratory: Cold Spring Harbor, NY, 2001.

(24) Jun, T.; Wennmalm, A. L-Arginine-induced hypotension in the rat: evidence that NO synthesis is not involved. *Acta Physiol. Scand.* **1994**, *152* (4), 385–390.

(25) Burns, K.; Martinon, F.; Esslinger, C.; Pahl, H.; Schneider, P.; Bodmer, J. L.; Di Marco, F.; French, L.; Tschopp, J. MyD88, an adapter protein involved in interleukin-1 signaling. *J. Biol. Chem.* **1998**, *273* (20), 12203–12209.

(26) Li, H.; Lin, X. Positive and negative signaling components involved in TNFα-induced NF-κB activation. *Cytokine* **2008**, *41* (1), 1–8.

(27) Sharon, N. Lectin receptors as lymphocyte surface markers. *Adv. Immunol.* **1983**, *34*, 213–298.

(28) Lombardi, L. M.; Brody, S. Circadian rhythms in *Neurospora crassa*: clock gene homologues in fungi. *Fungal Genet. Biol.* **2005**, *42* (11), 887–892.

(29) Wilson, L. M.; Idnurm, A.; Howlett, B. J. Characterization of a gene (sp1) encoding a secreted protein from *Leptosphaeria maculans*, the blackleg pathogen of *Brassica napus. Mol. Plant Pathol.* **2002**, *3* (6), 487–493.

(30) Pazzagli, L.; Cappugi, G.; Manao, G.; Camici, G.; Santini, A. Scala, A. Purification, characterization, and amino acid sequence of cerato-platanin, a new phytotoxic protein from *Ceratocystis fimbriata* f. sp. *platani. J. Biol. Chem.* **1999**, *274* (35), 24959–24964.

(31) Pan, S.; Cole, G. T. Molecular and biochemical characterization of a *Coccidioides immitis*-specific antigen. *Infect. Immun.* **1995**, *63* (10), 3994–4002.

(32) Hall, N.; Keon, J. P. R.; Hargreaves, J. A. A homologue of a gene implicated in the virulence of human fungal diseases is present in a plant fungal pathogen and is expressed during infection. *Physiol. Mol. Plant Pathol.* **1999**, *55* (1), 69–73.

(33) Zhu, H.; Nowrousian, M.; Kupfer, D.; Colot, H. V.; Berrocal-Tito, G.; Lai, H.; Bell-Pedersen, D.; Roe, B. A.; Loros, J. J.; Dunlap, J. C. Analysis of expressed sequence tags from two starvation, time-of-day-specific libraries of *Neurospora crassa* reveals novel clock-controlled genes. *Genetics* **2001**, *157* (3), 1057–1065.

(34) Bell-Pedersen, D.; Crosthwaite, S. K.; Lakin-Thomas, P. L.; Merrow, M.; Okland, M. The *Neurospora* circadian clock: simple or complex?. *Philos. Trans. R. Soc. London Ser. B−Biol. Sci.* **2001**, *356* (1415), 1697–1709.

(35) Temple, B.; Horgen, P. A. Biological roles for cerato-ulmin, a hydrophobin secreted by the elm pathogens, *Ophiostoma ulmi* and O-novo-ulmi. *Mycologia* **2000**, *92* (1), 1–9.

(36) Aderem, A.; Ulevitch, R. J. Toll-like receptors in the induction of the innate immune response. *Nature (London)* **2000**, *406* (6797), 782–787.

(37) Deetz, C. O.; Hebbeler, A. M.; Propp, N. A.; Cairo, C.; Tikhonov, I.; Pauza, C. D. γ interferon secretion by human Vγ2Vδ2 T cells after stimulation with antibody against the T-cell receptor plus the Toll-Like receptor 2 agonist Pam3Cys. *Infect. Immun.* **2006**, *74* (8), 4505–4511.

in a T1/T2 doubly transgenic mouse model for inhibiting infection of *Schistosoma mansoni. Toxicol. Appl. Pharmacol.* **2008**, *227* (2), 291–298.

Article

J. Agric. Food Chem., Vol. 57, No. 10, 2009   **4141**

(38) Hadley, J. S.; Wang, J. E.; Foster, S. J.; Thiemermann, C.; Hinds C. J. Peptidoglycan of *Staphylococcus aureus* upregulates monocyte expression of CD14, Toll-like receptor 2 (TLR2), and TLR4 in human blood: possible implications for priming of lipopolysaccharide signaling. *Infect. Immun.* **2005**, *73* (11), 7613–7619.

(39) Bulut, Y.; Faure, E.; Thomas, L.; Equils, O.; Arditi, M. Cooperation of Toll-like receptor 2 and 6 for cellular activation by soluble tuberculosis factor and *Borrelia burgdorferi* outer surface protein A lipoprotein: role of Toll-interacting protein and IL-1 receptor

signaling molecules in Toll-like receptor 2 signaling. *J. Immunol.* **2001**, *167* (2), 987–994.